Bui H. Hoang [a,b,*], Michael B.W. Fyhn [c], Jussi Hovikoski [c,d], Lars O. Boldreel [b], Nguyen Q. Tuan [a], Mai H. Dam [a], Hoang V. Long [a], Nguyen T. Tung [a], Lars H. Nielsen [c], Ioannis Abatzis [c]

[a] Vietnam Petroleum Institute, 167 Trung Kinh, Cau Giay, Hanoi, Viet Nam

[b] Department of Geosciences and Natural Resource Management, University of Copenhagen, Øster Voldgade 10, DK-1350, Copenhagen K, Denmark

[c] Geological Survey of Denmark and Greenland, GEUS, Øster Voldgade 10, 1350, Copenhagen K, Denmark

[d] Geological Survey of Finland (GTK), Vuorimiehentie 5, P.O. Box 96, FI 02151, Espoo, Finland

*Corresponding author: Bui H. Hoang (hoangbh.epc@vpi.pvn.vn)

Key points

- Hue Sub-basin, located in western Song Hong Basin, distinguishes in timing and structural development from the rest of the Song Hong Basin
- Hue Sub-basin opened in Late Oligocene – Early Miocene
- Transpression in northern Hue Sub-basin and northern Song Hong Basin could be effects from SE Asia-Australia collision

Abstract

Cenozoic strike-slip deformation and associated basin formation in Indochina provide critical clues on crustal response during India-Asia collision. Typically, Indochina is considered a rigid block during continental extrusion. We demonstrate that the Song Ca-Rao Nay Fault System (SCRNFS) in north central Vietnam and its offshore extension, the Hue Sub-basin, subdivided Indochina into discrete blocks. Using an integrated dataset including topographic maps, geologic maps, onshore fieldworks, and offshore seismic and well interpretation, the structural evolution of the SCRNFS and Hue Sub-basin is investigated. During Late Oligocene, the SCRNFS initiated with right-lateral motion, causing pull-apart onshore and Hue Sub-basin opening offshore. The End-Oligocene inversion affecting the northern Song Hong Basin also caused a major NE–SW reverse fault in the Hue Sub-basin. In Early Miocene, rifting resumed in the Hue Sub-basin with accelerated faulting and westward rift migration in the south. This is distinct from the Song Hong Basin, where the main rift period was Eocene(?) – Oligocene, and the Early Miocene only features mild extension. During latest Early Miocene – earliest Middle Miocene, the SCRNFS switched to left-lateral transpression. This caused inversion and prolonged uplift in the northern-most Hue Sub-basin. The inversion associated unconformity can be traced onshore where it separates a compositionally immature conglomerate from an overlying

quartz conglomerate. Left-lateral transpression in the Hue Sub-basin coincides with that in the Song Hong Basin and other inversion events across SE Asia. This may have been caused by Australia-SE Asia collision restricting escape movement of Indochina away from the India-Asia collision zone.

Keywords: Song Ca-Rao Nay Fault System, strike-slip, Indochina, extrusion, Hue Sub-basin

Introduction

According to extrusion tectonic models, large-scale strike-slip faults formed in response to the India-Eurasia collision that forced crustal blocks in SE Asia away from the collision zone (Tapponnier et al., 1986; Leloup et al., 2001) (Figure 1A). Some of these faults stretch for hundreds of kilometers from the collision zone into the South China Sea and control Cenozoic basin opening (Tapponnier et al., 1986; Leloup et al., 2001; Fyhn et al., 2009). These extrusion models assume that these crustal blocks behave rigidly, and that the subduction margin surrounding SE Asia can move freely to permit escape from the India-Asia collision zone. However, debates exist on whether these assumptions are valid, and thus whether extrusion tectonics can fully account for deformation in SE Asia (Wang and Burchfiel, 1997; Li et al., 2017; Pubellier and Morley, 2014).

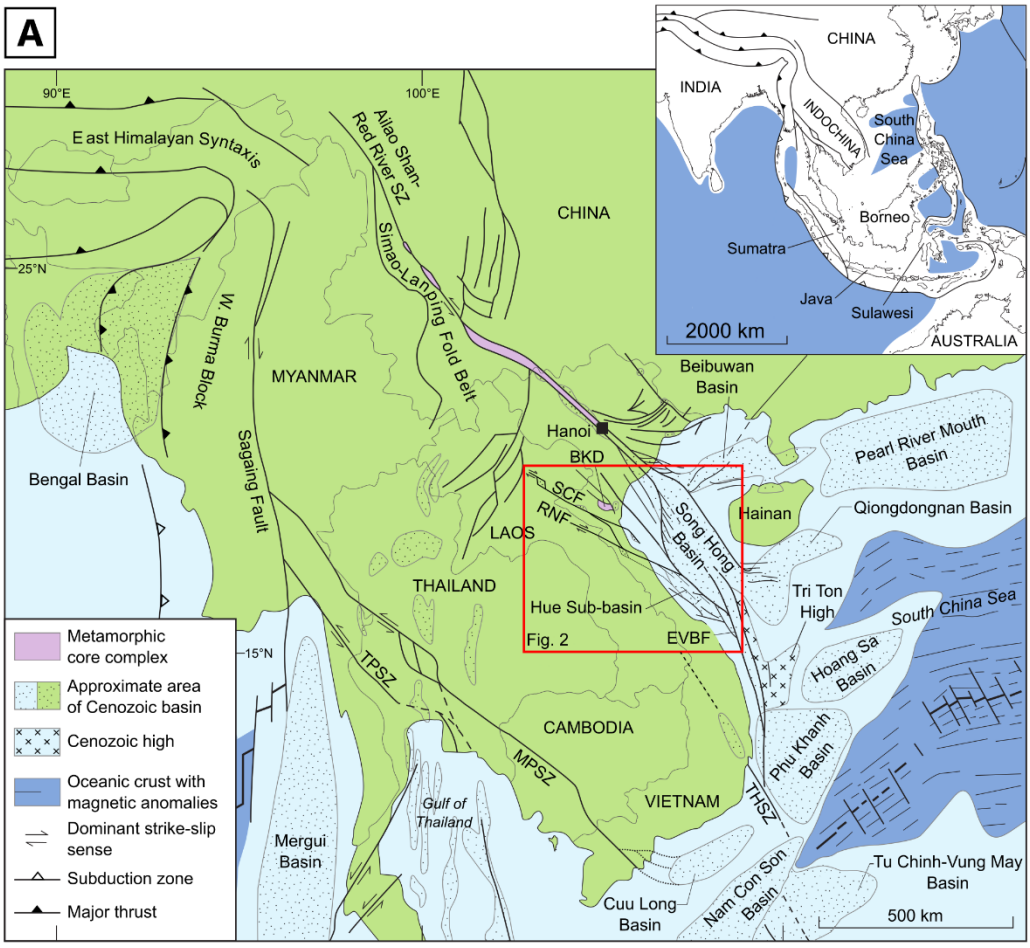
A
90°E
100°E
25°N
15°N
East Himalayan Syntaxis
Ailao Shan-Red River SZ
Simao-Lanping Fold Belt
W. Burma Block
Sagaing Fault
CHINA
MYANMAR
Bengal Basin
Beibuwan Basin
Hanoi
BKD
SCF
RNF
LAOS
THAILAND
Hue Sub-basin
Fig. 2
EVBF
Song Hong Basin
Hainan
Pearl River Mouth Basin
Qiongdongnan Basin
Tri Ton High
South China Sea
Hoang Sa Basin
Phu Khanh Basin
TPSZ
MPSZ
THSZ
CAMBODIA
VIETNAM
Gulf of Thailand
Mergui Basin
Cuu Long Basin
Nam Con Son Basin
Tu Chinh-Vung May Basin
500 km
INDIA
INDOCHINA
South China Sea
Borneo
Sumatra
Java
Sulawesi
AUSTRALIA
2000 km
Metamorphic core complex
Approximate area of Cenozoic basin
Cenozoic high
Oceanic crust with magnetic anomalies
Dominant strike-slip sense
Subduction zone
Major thrust

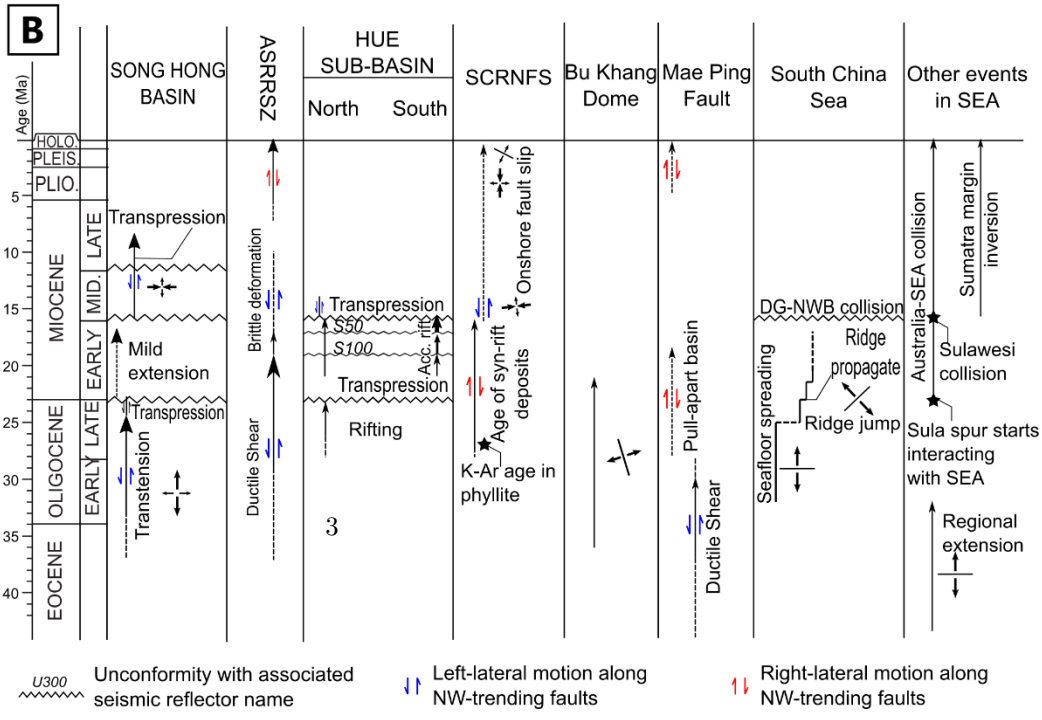
B
Age (Ma)
HOLO.
PLEIS.
PLIO.
MIOCENE
LATE
MID.
EARLY
OLIGOCENE
LATE
EARLY
EOCENE
5
10
15
20
25
30
35
40
SONG HONG BASIN
Transpression
Mild extension
Transpression
Transtension
ASRRSZ
Brittle deformation
Ductile Shear
HUE SUB-BASIN
North
South
Transpression
S50
S100
Acc. rift
Transpression
Rifting
SCRNFS
Onshore fault slip
Age of syn-rift deposits
K-Ar age in phyllite
Bu Khang Dome
Mae Ping Fault
Pull-apart basin
Ductile Shear
South China Sea
DG-NWB collision
Ridge propagate
Ridge jump
Seafloor spreading
Other events in SEA
Australia-SEA collision
Sumatra margin inversion
Sulawesi collision
Sula spur starts interacting with SEA
Regional extension
3
U300
Unconformity with associated seismic reflector name
Left-lateral motion along NW-trending faults
Right-lateral motion along NW-trending faults

Figure 1. A) Sketch of regional tectonic elements in Indochina and surrounding areas. BKD = Bu Khang Dome; EVBF = East Vietnam Boundary Fault; MPSZ = Mae Ping Shear Zone; RNF = Rao Nay Fault; SCF = Song Ca Fault; THSZ = Tuy Hoa Shear Zone; TPSZ = Three Pagodas Shear Zone. B) Summary of tectonic events in the study area. SCRNFS = Song Ca-Rao Nay Fault system.

Up until now, much focus has been on major shear zones such as the Ailaoshan-Red River Shear Zone (ASRRSZ) (Leloup et al., 2001), and its offshore extension – the Song Hong basin (Rangin et al., 1995; Fyhn and Phach, 2015; Fyhn et al., 2018). Much less are known about the Song Ca-Rao Nay Fault System (SCRNFS) located 300 km to the south of the ASRRSZ, and its offshore extension – the Hue Sub-basin (Figure 1A). The structural history of the SCRNFS and the Hue Sub-basin depicts the rapidly evolving deformation and stress pattern in Indochina during continental extrusion, exemplifying the role of extrusion tectonics in the deformation of SE Asia.

Our study provides details on the tectonic evolution of the SCRNFS and the Hue Sub-basin, based on onshore fieldworks and interpretation of offshore seismic and well data. We then link the geologic history of this area to tectonic events in the Song Hong Basin as well as other regional events in SE Asia.

Geologic settings

Regional geology

SE Asia is presently bounded by convergent margins: subduction to the south and east, and collision with Australia to the southeast (inset of Figure 1A). Cenozoic basins have formed over much of Sundaland, the continental core of SE Asia, and its margins. Basin opening has been attributed to either tectonic escape or trench pull/subduction roll-back (Tapponnier et al., 1986; Hall, 2012; Pubellier and Morley, 2014). Basin opening initiated in the Eocene and became widespread in the Oligocene, during which the subduction zones surrounding Sundaland behaved as free boundaries (Pubellier and Morley, 2014). Since the latest Oligocene, the Sula Spur, a northern continental promontory of Australia, started interacting with Sundaland to the southeastern end (Hall and Morley, 2004). In the Middle Miocene, the effect of Australia-SE Asia collision was felt across Sundaland, causing basin inversion in Sumatra, Java, Borneo and arguably the Gulf of Tonkin (Pubellier and Morley, 2014).

One of the largest strike-slip faults in SE Asia is the 1000 km long NW-trending ASRRSZ, located in mainland SE Asia (Figure 1A). Numerous studies on the ASRRSZ indicate three main deformation phases during the Cenozoic (Figure 1B): 1) a pre-shearing crustal thickening phase (Jolivet et al., 2001; Anczkiewicz et al., 2007); 2) a ductile left lateral shearing phase followed by brittle left-lateral motion (Leloup et al., 2001; Gilley et al., 2003; Palin et al., 2013); and 3) a right-lateral brittle deformation phase since the Late Neogene (Leloup et al., 2001; Fyhn and Phach, 2015). The timing of left-lateral motion is debated, but a

36–34 Ma onset age is generally preferred, and this is compatible with the basin opening in the Gulf of Tonkin (Leloup et al., 2001; Fyhn et al., 2018; Hoang et al., 2020). The termination of left-lateral motion is about 17 Ma by absolute dating methods (Leloup et al., 2001), but structural history of the offshore Song Hong Basin suggests continued left-lateral motion until the Late Miocene (See section 2.2).

In many of the extrusion models, Indochina behaves as a single rigid block and the estimate of left-lateral offset along the ASRRSZ varies significantly from several hundreds of kilometers to about 120 km (Leloup et al., 1995; Hall, 2002). However, compressional deformation in the Lanping-Simao terrane (Wang and Burchfiel, 1997) indicates significant internal deformation within Indochina. Through a comprehensive review of published paleomagnetic data in the region, Li et al (2017) suggest that Indochina can be divided into several microblocks, each with its own rotation amount during tectonic extrusion. Thus, the left-lateral displacement along the ASRRSZ may reduce from onshore to offshore.

Song Hong basin

The Song Hong Basin formed at the offshore continuation of the ASRRSZ in the Gulf of Tonkin (Figure 1A). The basin evolution is directly linked to Cenozoic strike-slip motion along the ASRRSZ (e.g. Tapponnier et al., 1986; Rangin et al., 1995; Fyhn et al., 2018; Hoang et al., 2020). The basin opened during the Eocene(?)–Oligocene associated with left-lateral trans-rotation of the Indochina Block (Hoang et al., 2020). The End-Oligocene inversion interrupted rifting as the Indochina block moved southeastward without any rotation relative to South China (Leloup et al., 2001; Hoang et al., 2020). After a minor phase of extension in the Early Miocene (Vu et al., 2017; Fyhn et al., 2018; Hoang et al., 2020), the northern part of the basin underwent major transpression in the Miocene (Rangin et al., 1995; Fyhn and Phach, 2015). The onset of left-lateral transpression is marked by a regional unconformity, dated as earliest Middle Miocene (Rangin et al., 1995; Andersen et al., 2005; Fyhn and Phach, 2015). A switch from left-lateral to right-lateral motion of the ASRRSZ was assigned to either the end of the Miocene (Rangin et al., 1995; Leloup et al., 2001), or Late Miocene (Fyhn and Phach, 2015).

Hue Sub-basin

The Hue Sub-basin comprises the central-western part of the Song Hong Basin (Figure 1 and Figure *2*A). The structure and tectonic history of the basin is little known. Zhu et al (2009) focused on the structural evolution of the main Song Hong Basin and only show a schematic view of the Cenozoic structure of the Gulf of Tonkin, which also includes the Hue Sub-basin. Morley (2013) assumed that the Hue Sub-basin and the Song Hong Basin formed concurrently. He used it to argue against a major left-lateral offset over the ASRRSZ since the

Song Hong Basin was suggested to form at a restraining bend of the ASRRSZ. Hoang et al (2020) disputed this view, and showed a seismic line through the Hue Sub-basin, indicating that the basin opened in the Late Oligocene–Early Miocene. Thus, the opening of the Hue Sub-basin partly overlaps with but is mostly younger than the main part of the Song Hong Basin.

Song Ca-Rao Nay Fault System

The SCRNFS is one of several large NW-trending shear zones in the Truong Son Belt, northern central Vietnam (Lepvrier et al., 1997; Tri and Khuc, 2011). The fault system consists of two main faults: the Song Ca Fault to the north and Rao Nay Fault to the south (Figure *2*A). These faults extend for more than 280 km from Laos into north-central Vietnam and further continue into the Hue Sub-basin in the Gulf of Tonkin (Figure *2*A). Based on kinematic and radiometric dating data, these faults underwent right-lateral strike-slip motion during the Early Triassic, and subsequently were overprinted by a Cretaceous thermal and deformational phase (Lepvrier et al., 1997). Further dating of a right-lateral shear zone in Ordovician–Silurian sedimentary phyllite along the Song Ca Fault (sample MX 166 on Figure *2*A) yielded 26.4 and 27.3 Ma K-Ar ages, suggesting a Cenozoic phase of right-lateral motion (Minh et al., 2012). This is consistent with ENE–WSW extensional motion on the Bu Khang Metamorphic Dome to the northeast (Figure *2*A), with radiometric ages in the 36–21 Ma range (Lepvrier et al., 1997; Jolivet, 1999; Nagy et al., 2000). Stress inversion analysis based on fault slip data indicates at least three later phases of Cenozoic brittle deformation on the SCRNFS, including a left-lateral, right-lateral and NE-SW extensional phase (Minh et al., 2012; Minh, 2014).

Along the SCRNFS, a series of small right-lateral pull-apart basins formed, such as the Muang Kham Trough, Khe Bo Trough and Huong Khe Trough (Thom, 2004; Tri and Khuc, 2011; Thom et al., 2013). These small troughs are filled by Oligocene–Miocene deposits of the Khe Bo Formation (Thanh and Khuc, 2011; Tri and Khuc, 2011) (Figure *2*B). The formation consists of breccia and conglomerate at the base grading upward to conglomerate, sandstone, siltstone, coaly shale and coal seams. Its age has been tentatively assigned to Oligocene–Middle Miocene based on similarity in floral assemblages and lithology to other coal-bearing deposits in northern Vietnam (Thanh and Khuc, 2011). Other Neogene deposits are also exposed as low hills near Dong Hoi city, attributed to the Dong Hoi Formation (Figure *2*C). They consist of conglomerate and gritstone interbedded with siltstone, containing abundant palynological assemblages (Thanh and Khuc, 2011).

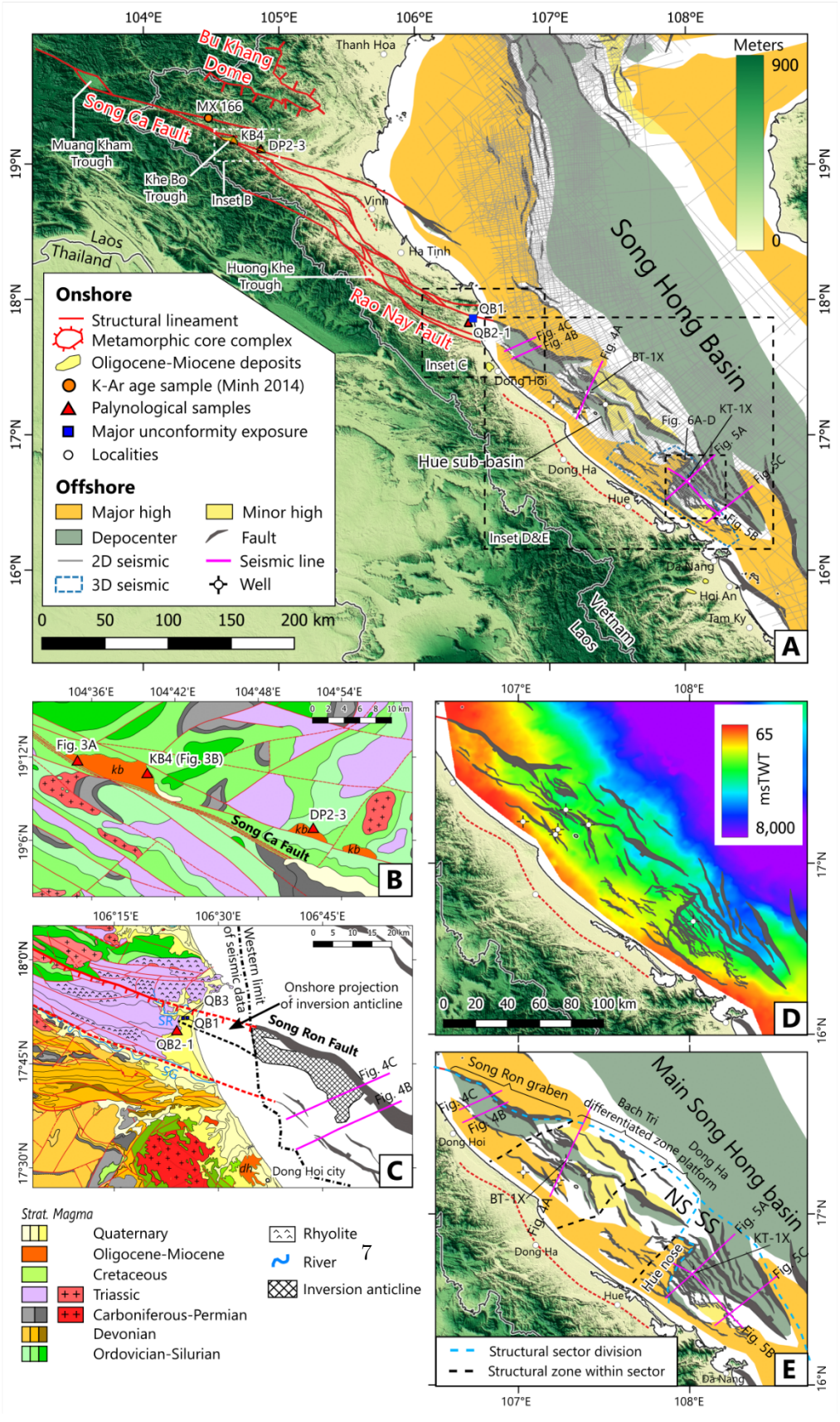
A
Bu Khang Dome
Song Ca Fault
MX166
KB4
DP2-3
Muang Kham Trough
Khe Bo Trough
Inset B
Huong Khe Trough
Rao Nay Fault
Laos
Thailand
Thanh Hoa
Vinh
Ha Tinh
Dong Hoi
Inset C
QB1
QB2-1
Fig. 4C
Fig. 4B
Fig. 4A
BT-1X
KT-1X
Fig. 6A-D
Fig. 5A
Fig. 5C
Fig. 5B
Song Hong Basin
Hue sub-basin
Dong Ha
Hue
Inset D&E
Da Nang
Hoi An
Tam Ky
Vietnam
Laos
Meters
900
0
Onshore
Structural lineament
Metamorphic core complex
Oligocene-Miocene deposits
K-Ar age sample (Minh 2014)
Palynological samples
Major unconformity exposure
Localities
Offshore
Major high
Minor high
Depocenter
Fault
2D seismic
Seismic line
3D seismic
Well
0 50 100 150 200 km
104°E
105°E
106°E
107°E
108°E
19°N
18°N
17°N
16°N
B
Fig. 3A
KB4 (Fig. 3B)
kb
DP2-3
Song Ca Fault
104°36'E
104°42'E
104°48'E
104°54'E
19°12'N
19°6'N
0 2 4 6 8 10 km
C
Western limit of seismic data
Onshore projection of inversion anticline
QB3
QB1
QB2-1
SR
SC
Song Ron Fault
Fig. 4C
Fig. 4B
dh
Dong Hoi city
106°15'E
106°30'E
106°45'E
18°0'N
17°45'N
17°30'N
0 5 10 15 20km
D
65
msTWT
8,000
0 20 40 60 80 100 km
107°E
108°E
17°N
16°N
E
Song Ron graben
Bach Tri differentiated zone
Dong Ha platform
Main Song Hong basin
NS
SS
Hue nose
Structural sector division
Structural zone within sector
Strat. Magma
Quaternary
Oligocene-Miocene
Cretaceous
Triassic
Carboniferous-Permian
Devonian
Ordovician-Silurian
Rhyolite
River
Inversion anticline

Figure 2. Characteristics of the SCRNFS and the Hue Sub-basin. A) Overview of the study area, with the field stations mentioned in the text. B&C) Geological map of the area around field stations along the Song Ca Fault (B) and the Rao Nay Fault (C). In inset C, the location of a major unconformity onshore (Figure 3F&G) is on strike with an end-of-Early-Miocene inversion anticline mapped offshore. kb= Khe Bo Formation; dh = Dong Hoi Formation; SG = Song Gianh River; SR = Song Ron River. D&E) Top pre-Cenozoic structural map and structural division of the Hue Sub-basin. NS = Northern Sector; SS = Southern Sector.

Database and methods

Onshore

We analyze regional structural lineaments based on geological maps, satellite maps and digital elevation model from Shuttle Radar Topography Mission. In Vietnam, geological maps at 1:200,000 scale cover the whole study area while in Laos, geological map at 1:1,500,000 scale are available (Tien et al., 2009). Fieldworks were done at five localities in north central Vietnam, in which three localities were sampled for palynological analysis (Figure *2*A). Integration of these data are done with the QGIS software.

For palynological analysis, standard preparation techniques were used. Firstly, 15 g of the sample was treated with 10% HCl in excess until all obvious reaction ceases to completely remove carbonate minerals. Next, the sample was treated with 40% HF to dissolve siliceous materials. A heavy liquid separation (specific gravity 2.2) to separate the organic and inorganic matter was performed by centrifugal process. Subsequently, the organic matter and filtrate were sieved by 5 µm nylon sieves (Lennie, 1968; Riding and Kyffin-Hughes, 2004; Traverse, 2007; Halbritter et al., 2018). Palynology slides were examined under a transmitted light microscope at 20X and 40X magnifications. For small fossils or a detailed focus on fossil structures, 100X oil immersion objective lenses were used. The fossil palynomorph assemblages were identified based on their structural and morphological characteristics (Anderson, 1963, 1964; Germeraad et al., 1968; Muller, 1968; Anderson and Muller, 1975; Morley, 1977, 1991, 2000; Mao and Foong, 2013; Morley and Morley, 2013). Quantitative analysis of the palynomorph assemblages is based on counts of full slides from all samples.

Offshore

The offshore dataset for this study includes about 50,000 km of 2D seismic data, 3200 km^2 of 3D seismic data and six exploration wells, courtesy of Vietnam Petroleum Institute (Figure *2*A). The seismic data were acquired by different operators since the 1980s, with varying processing parameters, thus the data quality varied from survey to survey. 2D line spacing varies from 2x4 km to 3x6 km, providing good coverage over the study area. A 3D survey covers a

significant fraction of the southern part of the study area, giving vital details and constraints to structural interpretations.

Six exploration wells are available in the study area, most of these are drilled on structural high, thus giving little information on syn-rift stratigraphy. Only two wells penetrated a significant portion of the Oligocene–Lower Miocene interval and offer important stratigraphic control for well-tie: BT-1X and KT-1X (Figure *2*A). In BT-1X, biostratigraphic analysis on cuttings and side wall cores were done by Shell in 1992. In KT-1X, the original biostratigraphic work was done by Shell in 1991, while a newer high-resolution biostratigraphic investigation was carried out by Vietnam Petroleum Institute in 2014.

Interpretations and results

Onshore

Structural characteristics of the SCRNFS

The SCRNFS are characterized by NW–SE fault strands that are clearly visible on satellite DEM data and confirmed by geological maps (Figure *2*A). There are two main fault orientations: N105–120E and N150–160E. The N105–120E fault strands can be up to 200 km long and together constitute the main traces of the SCRNFS. The N150–160E fault strands are 20–30 km long and form linkage segments or horsetail splays of the N105–120E fault strands. In the Vinh-Ha Tinh area, the main NW–SE strand of the Song Ca Fault splays into several NNW–SSE strands in a horsetail pattern (Figure *2*A). One strand of the Song Ca Fault continues into the offshore area and here confines a local half-graben. In the southern part, these fault strands connect with the Rao Nay Fault. Strands of the Rao Nay Fault continue offshore into the Hue Sub-basin.

Along the SCRNFS, basins form distinct lows on topographic maps. The largest of these are the Muang Kham and the Huong Khe troughs (Figure *2*A). The basins have a rhombic shape compatible with right-lateral pull-apart motion on the SCRNFS. Both the Muang Kham and the Huong Khe troughs are about 20–25 km long, which suggest an upper limit for right-lateral displacement. Smaller, isolated depressions of the Khe Bo Trough are also exposed along the Song Ca Fault (Figure *2*B).

Lithology and age of syn-rift deposits

We investigate Oligocene–Miocene deposits in small basins along the SCRNFS for lithology, geological relationship and age. Due to strong vegetation and heavy weathering, only a few sites have good exposures. In the Khe Bo Trough, the Khe Bo Formation consists of loosely consolidated, coarse-grained conglomerates located close to the main trace of the Song Ca Fault (Figure *3*A), and fine-grained coaly shales away from the main trace of the fault (Figure *3*B). The strata presumably form syn-rift deposits. Two samples from the coaly shale fa-

cies, KB 4 and DP 2-3 was investigated for their palynological content (Figure *2*B and Figure *3*B). Both samples are attributed to the Early–Middle Miocene based on the abundance of *Florschuetzia trilobata*, which disappeared at the end of the Middle Miocene, and the presence of *Florschuetzia levipoli*, which first appeared at the beginning of the Early Miocene (See Appendix 1 for more details).

Just south of the Song Ron River, loosely consolidated conglomerates and conglomeratic sandstones are exposed on the onshore continuation of the Song Ron Graben (Figure *2*C and Figure *3*C, F & G). Bedding is typically sub-horizontal or inclined a few degrees only. Meanwhile, the graben is floored by Triassic mud- and fine-grained sandstones, and the northern footwall is cored by earliest Triassic rhyolites (Figure *2*C and Figure *3*H). The conglomeratic clast composition is dominated by these Triassic rhyolites, mud- and fine-grained sandstones. The lithology and clast composition thus reflect a very local source and the unit is interpreted to have formed during active rifting.

We investigated 3 localities just south of the Song Ron River in details, namely QB1 to 3 (Figure *2*C). At locality QB3 (GPS N17.85909, E106.42509), basal part of the exposure consists of a ~3 m thick, broadly upward fining succession (see inset QB3 in Figure 3). The lower contact is not exposed, but the lowermost sediments comprise a poorly exposed, ~1.5m thick sub-unit showing interbedded, centimeter- to decimeter-thick granule and pebble rich gravel and stratified sandstone lenses. Weathered sandstone clasts and rare up to 10–15 cm subangular quartz clasts occur in the matrix. The gravelly sub-unit is sharply overlain by 1–2 m thick, upward fining, very fine-grained sandstone to siltstone-dominated succession. The deposits are characterized by millimeter-scale parallel lamination. Towards the top of the succession, roots and pedogenic alternation become common.

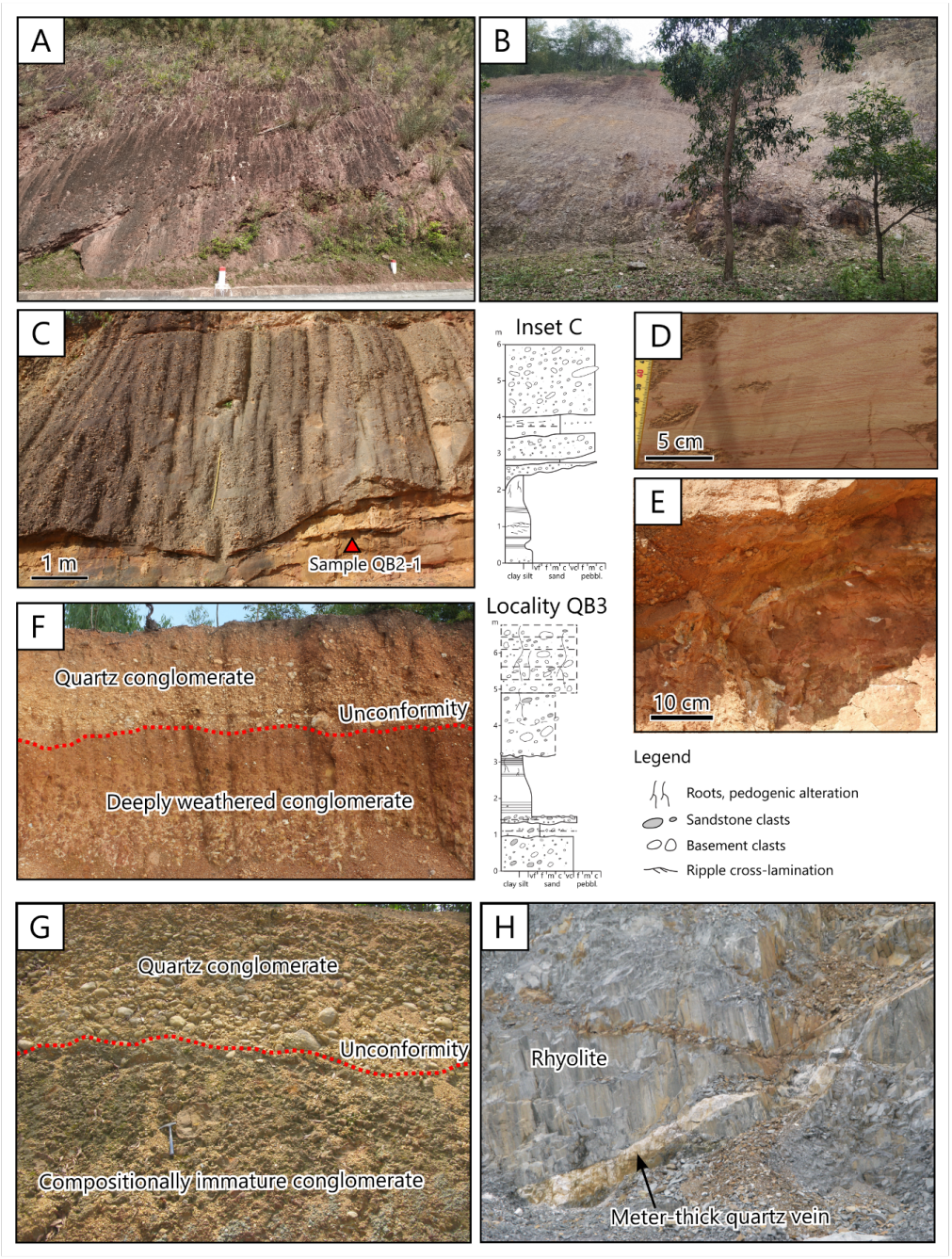
A
B
C
1 m
Sample QB2-1
Inset C
clay silt sand pebbl.
D
5 cm
E
10 cm
F
Quartz conglomerate
Unconformity
Deeply weathered conglomerate
Locality QB3
clay silt sand pebbl.
Legend
Roots, pedogenic alteration
Sandstone clasts
Basement clasts
Ripple cross-lamination
G
Quartz conglomerate
Unconformity
Compositionally immature conglomerate
H
Rhyolite
Meter-thick quartz vein

Figure 3. Field photos of Oligocene-Miocene deposits. A) Conglomerate in the Khe Bo Trough, Khe Bo Formation. B) Coaly shale in the Khe Bo Trough, Khe Bo Formation. Sample KB4 is taken for palynological analysis. C) A conglomeratic channel body truncating into root-bearing siltstone at locality QB2. Note the lensoidal form of the gravel interbeds. See sedimentological log ("inset C") for details. Sample QB2-1 is taken in the siltstone for palynological analysis. The succession is interpreted to be belong to the Dong Hoi Formation. D) Close-up of laminated and ripple cross-laminated siltstone facies at locality QB2. E) Close-up of the top of the siltstone facies showing common roots just below the erosional channel base. Locality QB2. F&G) An unconformity separating deeply weathered conglomerates of mixed origin and overlying quartz-dominated conglomerates at locality QB1. The outcrop in inset F is ~4 m high. The quartz conglomerate consists mainly of quartz pebbles up to 25 cm in size. H) Triassic rhyolite with thick quartz veins nearby could source the quartz conglomerate in F&G. The location of the samples and unconformity are on Figure 2.

At locality QB2 (GPS N17.829581, E106.3989966; Figure 3C), a similar upward fining silt-dominated succession is observed. Here, in addition to the general laminated character and root bearing top, small-scale current ripples occur in places (Figure 3D&E). The basal part of the unit is interpreted as fluvial. The alternating gravel and sand dominated lenses suggest flashy discharge and braided nature for the fluvial system. The abrupt change to silt dominated-grain size, parallel lamination, lack of wave generated structures and appearance of roots point to a change towards a protected, upward shallowing subaqueous environment. Considering the stratigraphic occurrence above fluvial sediments, the deposits may represent an abandoned river course.

In both localities QB2 and 3, the silt dominated interval is truncated by a gravel dominated unit up to 4 m thick. At locality QB2, the unit is well exposed along a N–S oriented outcrop, and shows undulating channel morphology, filled with a few m wide and some decimeters thick gravel lenses that are encased in medium to coarse grained sandstone interbeds (Figure 3C). The gravel is stratified and contain rounded basement pebbles and cobbles. The succession appears as aggradational and its upper contact is formed by the present day forest floor.

The channelized nature and interbedded gravel and sand lenses are interpreted to indicate alternating discharge and dominantly a braided river system. The undeformed nature of the siltstone as well as indications of pedogenic processes in its top (Figure 3E), suggest that there was a time gap between the emplacement of lacustrine siltstone and fluvial conglomerates, and that the surface may represent a sequence boundary.

On the 1:200,000 geologic map these deposits just south of the Song Ron River are indicated as Quaternary deposits (Figure 2C). These deposits are very similar lithologically to the deposits west of Dong Hoi City that were used to define the Dong Hoi Formation, which also consists of loosely consolidated conglomer-

ate and coarse-grained sandstone (Thanh and Khuc 2011). In addition, we collected sample QB 2-1 from the finest grained part of the succession for palynological analysis (Figure 3C). The sample's age is constrained to the Miocene based on the presence of *Florschuetzia levipoli* and absence of Pliocene-Quaternary marker palynomorphs (See Appendix 1 for more details). Thus, we reinterpret these deposits to belong to the Dong Hoi Formation.

At locality QB 1 (GPS N17.86009, E106.43331), the Dong Hoi Formation is unconformably overlain by a second, loosely consolidated conglomerate (Figure 3F&G). The older deposits include deeply weathered conglomerates of mixed origin (Figure 3F&G). The younger conglomerate is virtually entirely made from milky white quartz pebbles and decimeter to up to meter size quartz boulders. Bedding in the younger conglomerate is parallel to the unconformity and is inclined a few degrees to the east. These quartz clasts are considered to be sourced from milky quartz veins that cross-cut both the Triassic sediments flooring the graben and the Triassic rhyolites in the footwall nearby (Figure 3H). These veins are very common but only make up a minute fraction of the bulk of the Triassic. The virtual absence of Triassic rhyolite-, mud- and fine-grained sandstone clasts suggest their removal through long and pervasive syn-depositional weathering, leaving behind the erosion resistant quartz clasts. Thus, the unconformity separating the two conglomerates must represent a long hiatus.

Offshore

The top pre-Cenozoic structural map and structural division of the study area is illustrated on Figure *2*D & E. A major NE–SW reverse fault divide the study area into two main sectors: the Northern Sector and the Southern Sector (Figure *2*E). The following sub-sections first describe the regional correlation based on seismic and well data, and then describe these structural sectors and their variation through time.

Regional seismic and well correlation

Two wells BT-1X and KT-1X penetrate a significant portion of the Oligocene-Miocene syn-rift and were used as the main control for regional correlation. The well BT-1X, located in the Northern Sector, penetrates through the Lower Miocene, Upper Oligocene and into the Devonian carbonates, thus provides a relatively complete view on the Cenozoic syn-rift section. Meanwhile, the well KT-1X, located in the Southern Sector, penetrates more than 300 m of the Lower Miocene before terminating.

Based on the combined seismic and well data, we interpreted three main regional seismic horizons: Top pre-Cenozoic, Top Oligocene, and Top Early Miocene Unconformity (TEMU) (Figure 4 and Figure 5). In the Northern Sector, the Top pre-Cenozoic, Top Oligocene and TEMU is well constrained by biostratigraphic data from BT-1X, while in the Southern Sector only the TEMU is well constrained by biostratigraphic data from KT-1X (Figure 5). In the Southern Sec-

tor, 3D seismic data allows further separation of two major unconformities: S100 and S50 (Figure 5). S100 is an angular unconformity that separates the compresssionally folded succession below from the rifted succession above. S50 is an unconformity that divides the Early Miocene rift succession (S100 to TEMU) into two parts that are clearly observed on the 3D dataset. The lower part (S100–S50) is characterized by syn-rift wedges with slightly diverging reflector geometries and thickening toward syn-rift faults. The upper part (S50–TEMU) is characterized by pronounced syn-rift wedges with clear divergence of reflectors and strong thickness increase toward syn-rift faults.

Correlating S50 and S100 horizons from the southern part to the northern part on regional 2D data is very difficult due to differing tectonic and sedimentation styles, and due to a major structural high (the Hue Nose) separating the two areas. The biostratigraphic markers from BT-1X and KT-1X were converted to numerical ages. Then through linear extrapolation, the numerical age of the S100 and S50 horizons was estimated to independently test the regional correlation of these horizons (see section 4.2.4 for details).

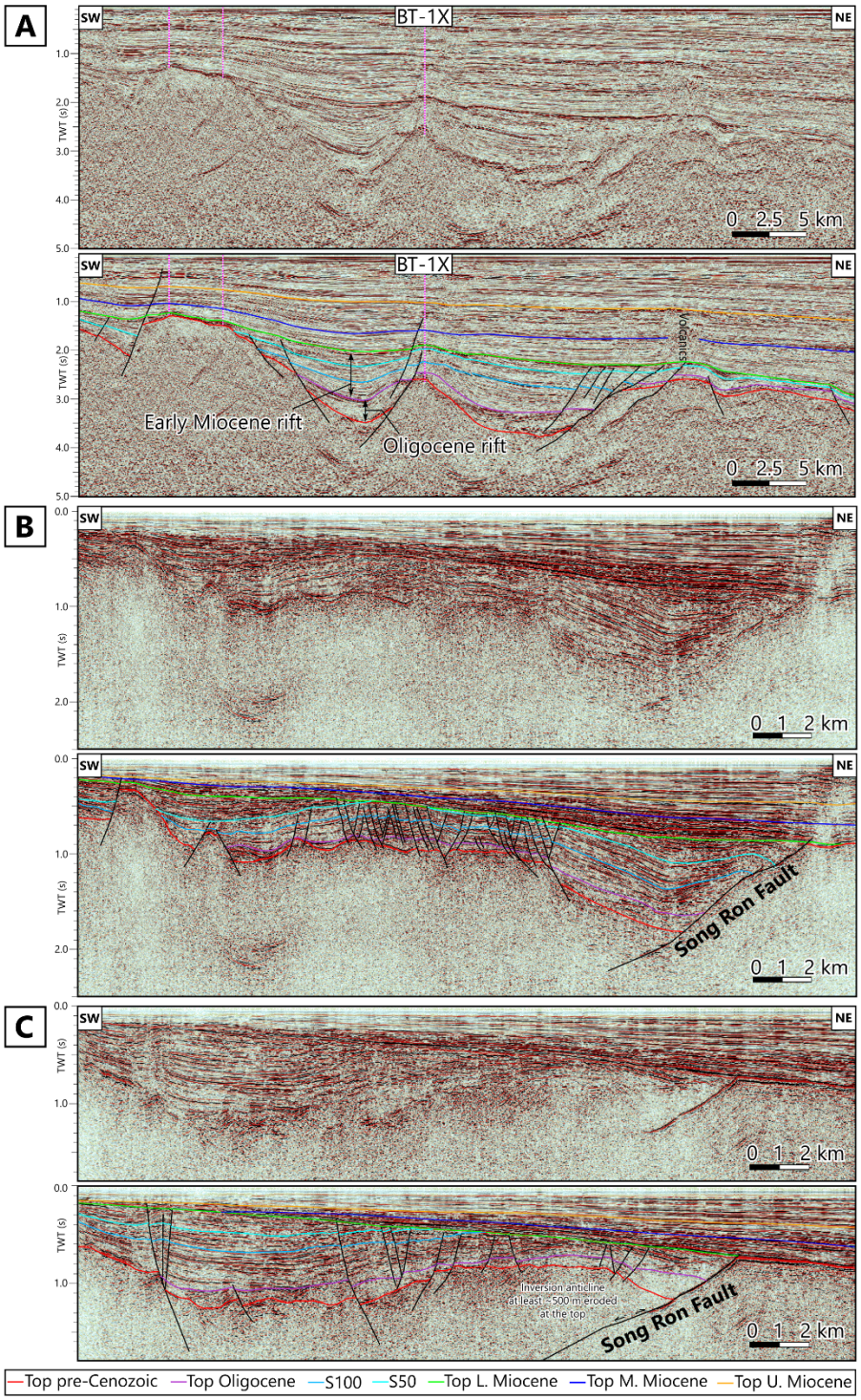
A
SW
BT-1X
NE
TWT (s)
0 2.5 5 km
Early Miocene rift
Oligocene rift
Volcanics
B
0 1 2 km
Song Ron Fault
C
Inversion anticline
at least ~500 m eroded
at the top
Top pre-Cenozoic
Top Oligocene
S100
S50
Top L. Miocene
Top M. Miocene
Top U. Miocene

Figure 4. Seismic profiles in the Northern Sector, Hue Sub-basin. A) Profile across the well BT-1X. B) Profile across the Song Ron graben. C) Profile across the northern part of the Song Ron graben where the End-of-Early Miocene transpression is observed. The line locations are indicated on Figure 2.

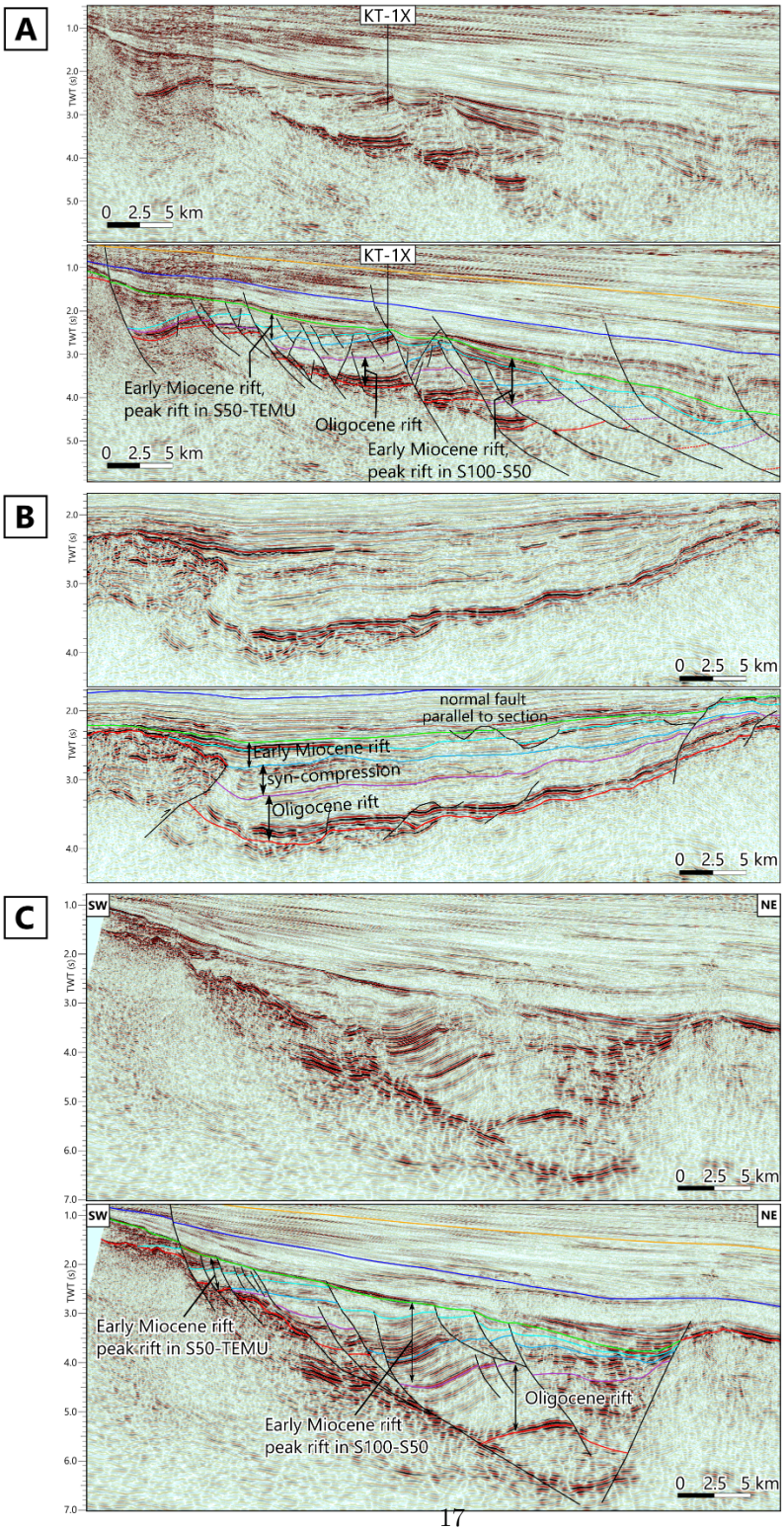
A
KT-1X
TWT (s)
0 2.5 5 km
KT-1X
Early Miocene rift,
peak rift in S50-TEMU
Oligocene rift
Early Miocene rift,
peak rift in S100-S50
0 2.5 5 km
B
0 2.5 5 km
normal fault
parallel to section
Early Miocene rift
syn-compression
Oligocene rift
0 2.5 5 km
C
SW
NE
0 2.5 5 km
SW
NE
Early Miocene rift
peak rift in S50-TEMU
Oligocene rift
Early Miocene rift
peak rift in S100-S50
0 2.5 5 km

Figure 5. Seismic profiles in the Southern Sector, Hue Sub-basin. A) Profile across the well KT-1X. B) Profile across the major NE-SW reverse fault. C) Profile in the southern part of the Southern Sector. The line locations are indicated on Figure 2. Keys to horizon color are on Figure 4.

Oligocene rift

From north to south, the Northern Sector includes the Song Ron Graben, the Bach Tri differentiated zone, the Dong Ha platform and the Hue Nose (Figure *2*E). The NW–SE trending Song Ron Graben lies on the direct continuation of the onshore SCRNFS (Figure *2*A). It is asymmetric in cross-section with the major west-dipping listric Song Ron Fault bounding the east (Figure 4B&C). On the southeastern end, the Song Ron fault changes to E–W strike as the graben transition into the Bach Tri differentiated zone. In contrast to the Song Ron Graben, the Bach Tri differentiated zone is characterized by a network of NW–SE normal faults, with most major faults dipping to the west. The Oligocene syn-rift is divided by these faults into wide syn-formal grabens (Figure 4A). Toward the south, faulting is much fewer on the Dong Ha platform and the Hue Nose with only one major fault that defines a large half-graben (Figure *2*E).

The Southern Sector is characterized by a dense network of NW-SE normal faults (Figure 5A). However, most of these faults were active not during the Oligocene but the Early Miocene rift instead (see section 4.2.4). The faults that were active during the Oligocene rift are major bounding faults more than 25 km in length (Figure *6*E). In deeper parts, the thick Oligocene syn-rift section seems well-developed (Figure 5C).

End-Oligocene compression

The End-Oligocene compression in the study area is indicated by the major NE–SW reverse fault that separate the Northern and Southern sectors (Figure *2*E and Figure 5B). The uplifted basement rock to the NW side of the fault forms the Hue Nose. On the 3D seismic profile across the fault (Figure 5B), the Oligocene sequence shows constant thickness, while the S100–Top Oligocene interval shows gradual thickening toward the reverse fault. In addition, truncation can be observed below the S100 surface close to the reverse fault, while away from the reverse fault, the S100 surface is arguably conformable. Furthermore, the interval above the S100 surface shows onlap onto the basement high uplifted by the reverse fault. Based on these observations, we interpret the reverse fault to be coeval with the S100—Top Oligocene interval.

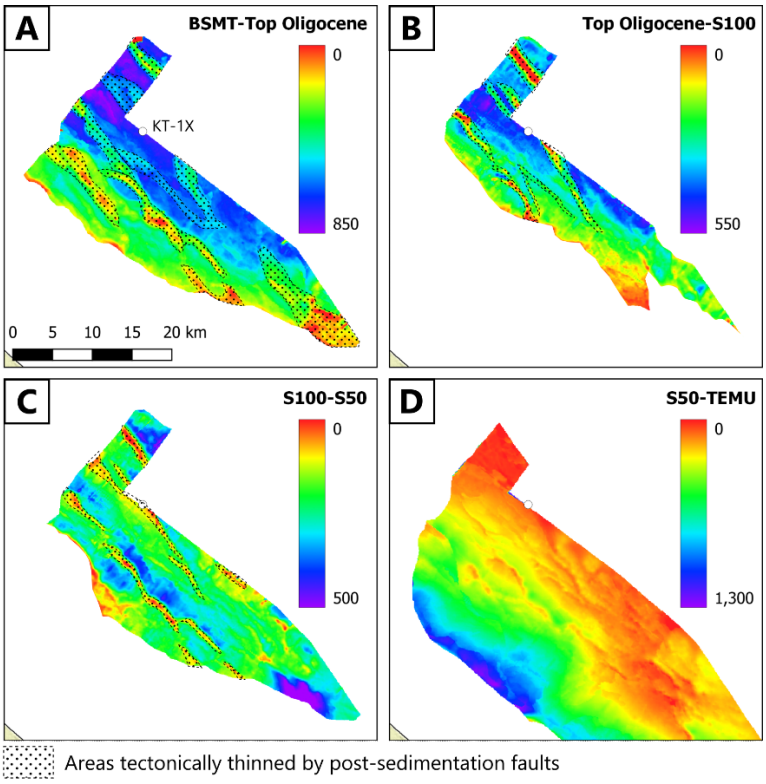
A
BSMT-Top Oligocene
0
850
KT-1X
0 5 10 15 20 km
B
Top Oligocene-S100
0
550
C
S100-S50
0
500
D
S50-TEMU
0
1,300
Areas tectonically thinned by post-sedimentation faults

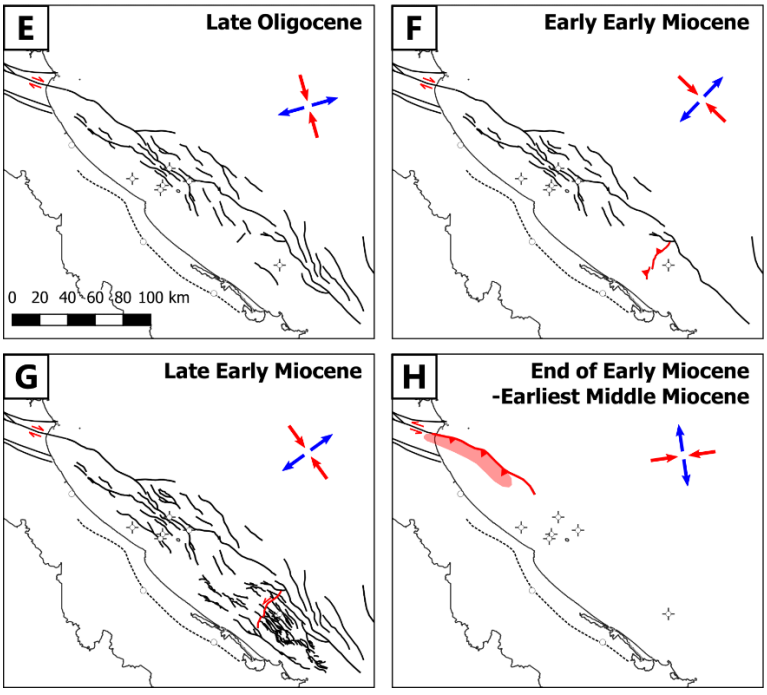
E
Late Oligocene
0 20 40 60 80 100 km
F
Early Early Miocene
G
Late Early Miocene
H
End of Early Miocene
-Earliest Middle Miocene

Figure 6. A-D) Isochron of major sequences in the Southern Sector in the area covered by 3D seismic data. Westward migration of the depocenter can be clearly observed from the interval S100-S50 and younger. E-H) Sketch of fault active timing in the study area and inferred stress regime.

On the isochron map of this area (Figure 6A-D), the Oligocene thickness shows thickening toward the main Song Hong Basin, except for areas where later Early Miocene rift faults with significant heave reduced the thickness of the Oligocene succession. The Top Oligocene–S100 isochron map shows two thickening trends: one is thickening toward the NW where the reverse fault is located, the other is thickening toward the NE into the main Song Hong Basin. The first thickening trend is consistent with the activity of the reverse fault, while the second thickening trend may reflect the thickening trend of the larger Song Hong Basin as it underwent weak extension during the Early Miocene.

Early Miocene rift

The characteristics of the Early Miocene rift differs between the Northern and the Southern sectors. Despite the difference, the Early Miocene rift is capped by the TEMU surface over the entire study area.

In the Southern Sector, the Early Miocene rift is clearly separated from the succession below by the S100 unconformity (Figure 5). Below the S100, the seismic reflectors are parallel with no change in thickness across most NW–SE normal faults. The syn-rift succession above the S100 can be further divided into two parts by the S50 unconformity, and the characteristics of these intervals change from east to west (Figure 5). In the eastern part, the main rift interval is S100–S50, characterized by dramatic thickening and strata divergence toward syn-rift faults. In contrast, in the western part, the S50–TEMU interval exhibits those characteristics of a main rift interval instead of the S100–S50. Thus, the rift center migrated westward from the S100–S50 interval to S50–TEMU interval. This rift migration can be clearly observed on the isopach maps as the depocenter migrate westward from below S100, to S100–S50 and finally S50–TEMU (Figure *6*A–D).

In the Northern Sector, the seismic reflector pattern of the Early Miocene rift is not as distinct from the Oligocene rift as seen in the Southern Sector. Seismic reflectors form wide synclines that follow the general shape of the Top Oligocene surface but decrease in amplitude upward (Figure 4A). This may indicate more gradual faulting activities and deposition in the Northern Sector. The westernmost trough on Figure 4A is filled by Lower Miocene deposits, with no confirmed Oligocene deposits. This may indicate westward migration of the rift center during the Early Miocene, similar to what is observed in the Southern Sector.

Biostratigraphic data in KT-1X and BT-1X offers indirect numerical age control for the S50 and S100 seismic horizon. In KT-1X, The Middle to Early Miocene boundary is interpreted at 3222 m based on the lower boundary of the *Florschuetzia semilobata* subzone and the upper boundary of the *Florschuetzia*

levipoli zone. Following Gradstein et al. (2020), this suggests an age of around 16 Ma at 3222m. The top of the *Florschuetzia trilobata* zone, which ends in the earliest Burdigalian, is at 3459 m. Following Gradstein et al. (2020), this suggests an age of around 20 Ma at 3459 m. Assuming a simple uninterrupted and linear burial history, the age of the S50 and S100 seismic horizon could be assigned around 17 Ma and 19 Ma in KT-1X, respectively (Table 1). With similar assumption but for the Top Early Miocene and Top Oligocene marker in BT-1X located in the Northern Sector, the S50 and S100 seismic horizons tied from the south around the Hue Nose are found to have similar numerical age (Table 1). Due to the presence of intra-Burdigalian unconformities and differing rift patterns in the Northern Sector and Southern Sector as well as evolving sedimentation rate through time, we hesitate to constrain ages more than the upper Burdigalian for S50 and mid-Burdigalian for S100.

Table 1. Numerical age estimate of the S50 and S100 horizon in KT-1X and BT-1X, assuming linear and uninterrupted burial history in both wells.

Well	Marker	Depth (m)	Age (Ma)	Note
KT-1X	Top LMIO	3222	15.97	VPI report
KT-1X	S50	3264	16.68	Approximate depth from seismic; age extra
KT-1X	S100	3382	18.69	Approximate depth from seismic; age extra
KT-1X	Top Florschuetzia trilobata	3459	20	VPI report; ends at earliest Burdigalian
BT-1X	Top LMIO	2420	15.97	Shell report
BT-1X	S50	2564	16.79	Approximate depth from seismic; age extra
BT-1X	S100	3118	19.92	Approximate depth from seismic; age extra
BT-1X	Top OLI	3667	23.03	Shell report

End of Early Miocene transpression

The end of Early Miocene transpression is only observed in the northern part of the Song Ron Graben (Figure 4C). In this area, the syn-rift succession close to the Song Ron Fault has been uplifted and folded into a major anticline with the top truncated by the TEMU. Since erosion and truncation occurred across the top and on the flank of the anticline against the Song Ron Fault, this could not be a simple rollover fold created by extension. Thus, we interpret this to be a compressional feature resulted from the inverted movement across the Song Ron Fault.

The extent of the inversion-induced uplift and truncation manifests as a NW–SE trending elongated area parallel to the Song Ron Fault (Figure *2*C). The onshore locality QB 1, where the unconformity between dominantly quartz conglomerate and the underlying compositionally immature conglomerate of the Dong Hoi Formation is observed, is on strike with this inversion anticline (Figure *2*C). The southward extent of this inversion anticline is not clear, as it is more difficult to distinguish it from extension-related roll-over fold (Figure 4B).

Discussion

Timing of SCRNFS right-lateral motion and linking with basin formation

Strands of the SCRNFS can be traced from onshore to offshore. The orientation of faults in the Hue Sub-basin is about 20 degrees clockwise from the trend of the main traces of the SCRNFS (Figure 7A). Therefore, the Hue Sub-basin is located in the extensional quadrant (Kim and Sanderson, 2006) at the end of the SCRNFS during right-lateral motion. Combined with their concurrent timing, we interpret that extension in the Hue Sub-basin is associated with right-lateral motion on the SCRNFS.

Palynological analysis of two samples (sample KB 4 and DP 2-3) indicate an Early–Middle Miocene age range for the Khe Bo Formation and thus for the right-lateral pull-apart troughs. This is consistent with the assessment by Thanh and Khuc (2011) based on comparison with coal-bearing deposits with similar lithology and palynological assemblages in northern Vietnam. In addition, Minh (2014) provided a syn-kinematic K-Ar age of 26.4 and 27.3 Ma (Late Oligocene) for phyllite within the Song Ca Shear Zone. Thus right-lateral motion along the SCRNFS started in the Late Oligocene and continued to sometime in the Early–Middle Miocene.

The close structural relationship between the SCRNFS and the offshore Hue Sub-basin suggests their concurrent timing. In addition, the end of rifting in the Hue Sub-basin is at the end of the Early Miocene. Furthermore, palynological analysis of one sample in the syn-kinematic Dong Hoi Formation (sample QB 2-1) yielded a Miocene age. This sample is located on the onshore continuation of the Song Ron Graben, and its age is consistent with the age of the Hue Sub-basin syn-rift timing. Therefore, right-lateral motion along the SCRNFS can be assigned to Late Oligocene–Early Miocene. The right-lateral pull-apart basins such as the Muang Kham Trough and the Huong Khe Trough probably also formed during this time.

This right-lateral timing is partly coeval with Oligocene ENE–WSW extension on the Bu Khang dome (Lepvrier et al., 1997; Jolivet, 1999; Nagy et al., 2000). The inferred ENE–WSW minimum principal stress on the Bu Khang Dome is also consistent with right-lateral motion along the SCRNFS.

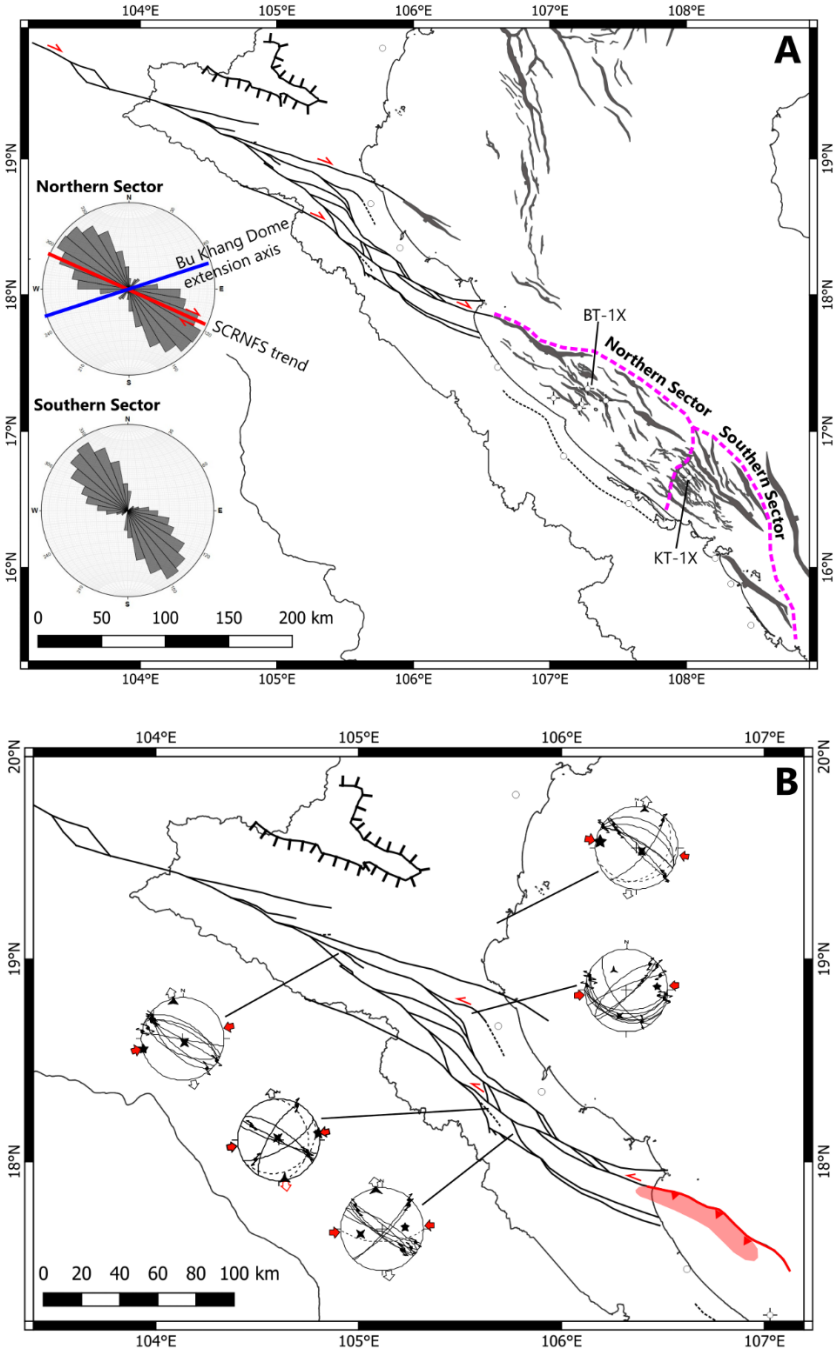

Figure 7. A) Fault trend in the Hue Sub-basin and comparison with that of the

SCRNFS. B) Fault slip data adapted from Minh (2014).

SCRNFS left-lateral motion and local basin inversion

Inversion at the end of the Early Miocene is observed in the northwestern end of the Hue Sub-basin. The inversion area trends NW–SE and is most pronounced close to the Song Ron Fault that defines the Song Ron Graben (Figure *2*C and Figure *6*H). The inversion caused significant uplift and erosion, and the TEMU denotes a prolonged hiatus. The inversion unconformity is interpreted to crop out onshore at the QB 1 locality forming the boundary between the quartz conglomerate (above) and the Dong Hoi Formation below, consistent with the prolonged weathering observed at the unconformity (Figure 3F&G). The gentle eastward inclination of the unconformity onshore mimics the inclination observed from seismic data in the offshore.

Inversion on the NW–SE trending Song Ron fault probably indicates a left-lateral phase of motion on the SCRNFS. This phase of motion is observed in fault kinematic data onshore (Figure 7B) (Minh et al., 2012; Minh, 2014). Since the effects of the inversion is only observed locally in the basin, the left-lateral offset was presumably small compared to the right-lateral offset.

Hue Sub-basin vs Song Hong Basin rift characteristics and timing

The Hue Sub-basin was previously perceived as part of the Song Hong Basin having a similar tectonic history (Morley, 2013). However, this study shows that the Hue Sub-basin's structural development is distinct from that of the rest of the Song Hong Basin. Firstly, the main Song Hong Basin lies on the direct continuation of the onshore left-lateral ASRRSZ with hundreds of kilometers of offset responsible for its opening, while the Hue Sub-basin lies on the direct continuation of the onshore right-lateral SCRNFS with tens of kilometers of offset at the most (section 4.1.1). Secondly, the main rifting period of the Song Hong Basin occurred during the Eocene (?)–Oligocene, and the Early Miocene only features mild extension (Vu et al., 2017; Fyhn et al., 2018; Hoang et al., 2020; Lei et al., 2021). Meanwhile, the main rifting period of the Hue Sub-basin occurred in the Early Miocene, with accelerated rifting and westward migration of the rift center toward the latter part of the Early Miocene.

The end-Oligocene inversion is a regional event that affected the northern Song Hong basin (Fyhn et al., 2018; Hoang et al., 2020). This event is recorded in the Hue Sub-basin as a prominent NE–SW reverse fault that separates the Northern Sector from the Southern Sector. Thus, the end-Oligocene inversion may have had a more regional effect than previously thought.

The onset of transpression following the Early Miocene transtension in the northern Song Hong basin is associated with a major angular unconformity, dated as earliest Middle Miocene in age (Rangin et al., 1995; Andersen et al., 2005; Fyhn

and Phach, 2015). This is coeval with the pulse of left-lateral transpression, uplift and erosion associated with inversion in the northern Song Ron Graben. Miocene transpression was more long-lived in the northern Song Hong basin. The overlap in timing suggests a common mechanism behind the left-lateral transpression of both basins.

Implications on Indochina extrusion

Existing tectonic reconstructions assume the portion of Indochina lying between the ASRRSZ and the Mae Ping fault zone to have behaved as a single rigid block, which serves as a good first-order approximation (Hall, 2012; Mazur et al., 2012). The motions on the SCRNFS documented here indicates a second order division of the Indochina block into at least two micro blocks. But Indochina may be composed by as much as four Cenozoic micro-blocks parted by the Mae Ping and the Tuy Hoa shear zones in the south (Nielsen et al., 2007; Fyhn et al., 2009; Vu et al., 2017; Schmidt et al., 2019) and the SCRNFS in the north. The SCRNFS is distinct from the Mae Ping and the Tuy Hoa shear zones in that its Cenozoic history initiated with right-lateral motion in contrast with the left-lateral displacement taking place over the two shear zones in the south.

Interaction between the migrating India-Eurasia collision front and the boundary condition on the subduction margin surrounding SE Asia is very complex and variable through time (Pubellier and Morley, 2014). Earlier tectonic escape models assumed the subduction margin surrounding SE Asia to be a free boundary, and extrusion tectonics to have played a dominant role in basin formation in SE Asia (Tapponnier et al., 1986). Huchon et al. (1994) further assumed that the present-day stress field, where the trajectories of maximum horizontal stress radiate outward from the East Himalayan Syntaxis, stayed relatively constant through time and only migrate northward with India. According to Huchon et al. (1994), one would expect a change from left-lateral to right-lateral motion to occur over NW-SE strike-slip faults. Furthermore, the change in motion was suggested to decrease in age from south to north as India migrate northward. When comparing the timing of major strike-slip faults in Indochina such as the ASRRSZ, the Mae Ping fault as well as the SCRNFS, this study partly supports this model (Figure 1B).

During the Eocene (?)–Early Oligocene, the Hue Sub-basin had not opened while the Song Hong Basin already underwent extension associated with left-lateral motion on the ASRRSZ (Figure 8). During this time, the position of the India-Asia collision front would have induced NE–SW to E–W trending maximum horizontal stress in northern Indochina (Huchon et al., 1994), thus inducing left-lateral motion on NW–SE faults. However, the SCRNFS follows older Indosinian trends of the Truong Son Belt (Lepvrier et al., 1997) with right step-overs between NW–SE fault segments. Thus, left-lateral motion on these fault trends would cause lock-up and either no motion, or compression at the step-overs, rather than basin opening. The Song Hong Basin is also situated at a restraining bend of the ASRRSZ (Morley, 2013), however the combined

motion of clockwise rotation and SE-ward translation of Indochina permitted basin opening (Leloup et al., 2001; Hoang et al., 2020).

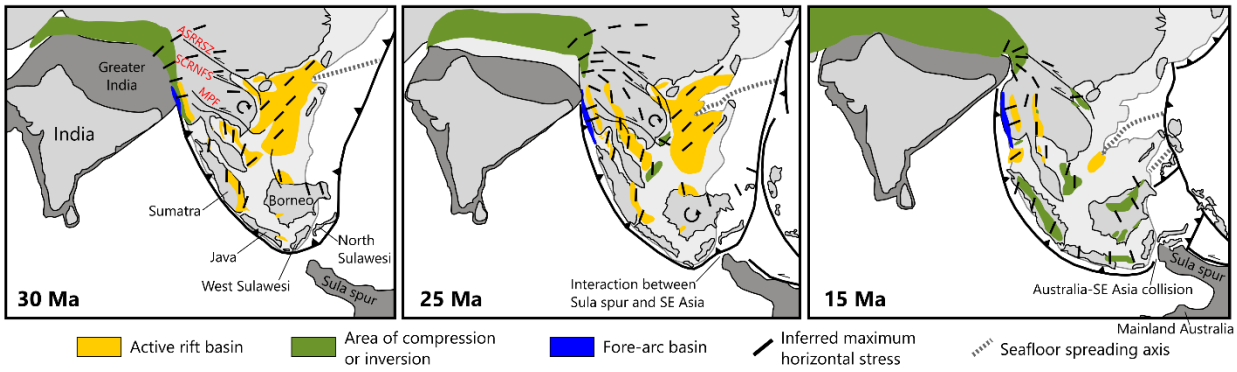

Figure 8. Tectonic reconstruction of Southeast Asia during the Oligocene-Miocene. MPF = Mae Ping Fault. Modified from Pubellier and Morley (2014).

During the Late Oligocene–Early Miocene, the Hue Sub-basin opened associated with right-lateral motion on the SCRNFS, while the Song Hong Basin underwent mild extension associated with left-lateral motion on the ASRRSZ (Rangin et al., 1995; Fyhn et al., 2018). During the Late Oligocene, the extension axis of the coeval Bu Khang Dome and fault trends offshore suggest ENE–WSW minimum principal stress and NNW–SSE maximum principal stress (Figure *6*E). During the Early Miocene, fault trends in the Hue Sub-basin suggest NE-SW minimum principal stress and NW–SE maximum principal stress (Figure *6*G). Apparently, both the ASRRSZ and SCRNFS are NW-trending, yet they had different strike-slip motion at the same time. According to Huchon et al. (1994) model, this could be explained by the position of the East Himalayan Syntaxis such that the ASRRSZ lied in the NNE–SSW maximum horizontal stress region, while the SCRNFS lied in the NW–SE maximum horizontal stress region (Figure 8).

However, Huchon et al. (1994)'s model does not explain the end–Early Miocene transpression well, where the SCRNFS underwent left-lateral motion again after right-lateral motion in the Late Oligocene–Early Miocene. This transpression event occurred sometime in the latest Early Miocene–early Middle Miocene, which coincided with left-lateral transpression in the northern Song Hong Basin (Rangin et al., 1995; Andersen et al., 2005; Fyhn and Phach, 2015). The Middle Miocene is also a significant time in the tectonic history of SE Asia, where the switch from extension to compression occur in many areas, in particular the Sumatra-Java margin inversion, Dangerous Grounds-NW Borneo collision, and Australia-SE Asia collision (Pubellier and Morley, 2014) (Figure 8). Thus, the free boundary assumption during this time is no longer valid, and compression forces from the above-mentioned margins could incur changes in regional stress-field in northern Indochina. Without a free boundary, the extrusion and rotation of Indochina could be significantly reduced. This is consistent with

observed transpression on restraining bends associated with left-lateral motion on NW–SE faults, particularly offshore in the northern Song Hong Basin and the northern Hue Sub-basin. Onshore, this transpression caused a major unconformity between the quartz conglomerate above and the underlying Dong Hoi Formation observed at station QB 1.

Conclusion

Using an integrated dataset consisting of topographic maps, geologic maps, onshore fieldwork and offshore 2 and 3-D seismic and well data, we provided details on the structural characteristics of the lesser-known SCRNFS and its offshore extension, the Hue Sub-basin. These observations allow us to infer a geologic history of the study area and relate them to regional events in SE Asia. Cenozoic right-lateral motion along the SCRNFS initiated in the Late Oligocene, as recorded by radiometric dating as well as the age of syn-rift deposits in pull-apart troughs onshore and in the Hue Sub-basin offshore. The End-Oligocene inversion event that affected the northern Song Hong Basin manifests in the Hue Sub-basin as a major NE–SW reverse fault that divides the sub-basin into a northern and southern sector. Basin formation continued and peaked in the Early Miocene in the Hue Sub-basin, with accelerated rifting and westward migration of the rift center that is most pronounced in the Southern Sector. This contrasts with the main Song Hong Basin where the main rift period was during the Eocene(?)–Oligocene, and the Early Miocene only featured mild extension. Thus, the Hue Sub-basin, despite overlap in basin formation timing, is distinct from the Song Hong Basin.

A mild inversion event during the latest Early Miocene–earliest Middle Miocene is observed in the northern-most part of the Hue Sub-basin and its onshore continuation. Close to the offshore Song Ron Fault, inversion resulted in a broad anticline truncated along the base of the Middle Miocene, indicating inverted movement across the fault and prolonged uplift and non-deposition across the anticline top. Onshore, the erosion and prolonged hiatus are observed as an unconformity between almost exclusively quartz conglomerate above and compositionally immature conglomerate of the Dong Hoi Formation below. The geometry of the inversion structure suggests left-lateral motion across the SCRNFS, which is consistent with onshore fault slip data. This event corresponds to left-lateral transpression in the northern Song Hong basin, as well as widespread compression events elsewhere in SE Asia. This could reflect the effect of the Australia-SE Asia collision restricting escape movement from the India-Asia collision front. Therefore, left-lateral transpression occurs along restraining bends of NW–SE faults such as in the northern Song Hong basin and in the northern part of the Hue Sub-basin.

Acknowledgement

The study is the outcome of a joint-research project between the Vietnam Petroleum Institute (VPI) and the Geological Survey of Denmark and Greenland (GEUS). We express our gratitude towards PetroVietnam and VPI for funding the PEXMOD project, from which this research originated; the funding of field trips to north central Vietnam and palynological analysis; access to seismic and well data; as well as permission to publish the work. PetroVietnam holds the rights to seismic and well data used in the study, parties interested in accessing these data can contact Tung N.T. at tungnt@vpi.pvn.vn. BHH acknowledges the University of Copenhagen, Denmark for housing his Ph.D., and Aarhus University, Denmark for accommodating part of his research stay.

References

Anczkiewicz, R., Viola, G., Müntener, O., Thirlwall, M.F., Villa, I.M., Quong, N.Q., 2007. Structure and shearing conditions in the Day Nui Con Voi massif: Implications for the evolution of the Red River shear zone in northern Vietnam. Tectonics 26, n/a-n/a. https://doi.org/10.1029/2006TC001972Andersen, C., Mathiesen, a, Nielsen, L.H., Tiem, P.V., Petersen, H.I., Dien, P.T., 2005. Distribution of source rocks and maturity modelling in the northern Cenozoic Song Hong Basin (Gulf of Tonkin), Vietnam. Journal of Petroleum Geology 28, 167–184. https://doi.org/10.1111/j.1747-5457.2005.tb00078.xAnderson, J.A.R., 1964. The structure and development of the peat swamps of Sarawak and Brunei. The Journal of Tropical Geography, The Journal of Tropical Geography. - Singapore : Univ., ISSN 0022-5290, ZDB-ID 799565-9. - Vol. 18.1964, p. 7-16 18, 7–16.Anderson, J.A.R., 1963. The Flora of the Peat Swamp Forests of Sarawak and Brunei, including a catalogue of all recorded species of flowering plants, ferns and fern allies. The Gardens' Bulletin, Singapore 20, 131–228.Anderson, J.A.R., Muller, J., 1975. Palynological study of a holocene peat and a miocene coal deposit from NW Borneo. Review of Palaeobotany and Palynology 19, 291–351. https://doi.org/10.1016/0034-6667(75)90049-4Barckhausen, U., Engels, M., Franke, D., Ladage, S., Pubellier, M., 2014. Evolution of the South China Sea: Revised ages for breakup and seafloor spreading. Marine and Petroleum Geology 58, 599–611. https://doi.org/10.1016/j.marpetgeo.2014.02.022Briais, A., Patriat, P., Tapponnier, P., 1993. Updated interpretation of magnetic anomalies and seafloor spreading stages in the south China Sea: Implications for the Tertiary tectonics of Southeast Asia. Journal of Geophysical Research: Solid Earth 98, 6299–6328. https://doi.org/10.1029/92JB02280Fyhn, M.B.W., Boldreel, L.O., Nielsen, L.H., 2009. Geological development of the Central and South Vietnamese margin: Implications for the establishment of the South China Sea, Indochinese escape tectonics and Cenozoic volcanism. Tectonophysics 478, 184–214. https://doi.org/10.1016/j.tecto.2009.08.002Fyhn, M.B.W., Cuong, T.D., Hoang, B.H., Hovikoski, J., Olivarius, M., Tuan, N.Q., Tung, N.T., Huyen, N.T., Cuong, T.X., Nytoft, H.P., Abatzis, I., Nielsen, L.H.,

2018. Linking Paleogene rifting and inversion in the northern Song Hong and Beibuwan basins, Vietnam, with left-lateral motion on the Ailao Shan-Red River Shear Zone. Tectonics 37, 2559–2585. https://doi.org/10/gdvjk8Fyhn, M.B.W., Phach, P.V., 2015. Late Neogene structural inversion around the northern Gulf of Tonkin, Vietnam: Effects from right-lateral displacement across the Red River fault zone: Inversion in the northern Gulf of Tonkin. Tectonics 34, 290–312. https://doi.org/10.1002/2014TC003674Germeraad, J.H., Hopping, C.A., Muller, J., 1968. Palynology of tertiary sediments from tropical areas. Review of Palaeobotany and Palynology, Palinology of Tertiary Sediments from Tropical Areas 6, 189–348. https://doi.org/10.1016/0034-6667(68)90051-1Gilley, L.D., Harrison, T.M., Leloup, P.H., Ryerson, F.J., Lovera, O.M., Wang, J.-H., 2003. Direct dating of left-lateral deformation along the Red River shear zone, China and Vietnam. Journal of Geophysical Research: Solid Earth 108. https://doi.org/10/d3n42mGradstein, F.M., Ogg, J.G., Schmitz, M.D., Ogg, G.M., 2020. Geologic Time Scale 2020. Elsevier. https://doi.org/10.1016/C2020-1-02369-3Halbritter, H., Ulrich, S., Grímsson, F., Weber, M., Zetter, R., Hesse, M., Buchner, R., Svojtka, M., Frosch-Radivo, A., 2018. Methods in Palynology. Illustrated Pollen Terminology. Springer, Cham, 97–127.Hall, R., 2012. Late Jurassic-Cenozoic reconstructions of the Indonesian region and the Indian Ocean. Tectonophysics 570–571, 1–41. https://doi.org/10.1016/j.tecto.2012.04.021Hall, R., 2002. Cenozoic geological and plate tectonic evolution of SE Asia and the SW Pacific. Journal of Asian Earth Sciences 20, 353–431.Hall, R., Morley, C.K., 2004. Sundaland basins. In: Clift, P., Kuhnt, W., Wang, P., Hayes, D. (Eds.), Continent-Ocean Interactions Within East Asian Marginal Seas. American Geophysical Union, Washington, D. C., 55–85. https://doi.org/10.1029/149GM04Hoang, B.H., Fyhn, M.B.W., Cuong, T.D., Tuan, N.Q., Schmidt, W.J., Boldreel, L.O., Anh, N.T.K., Huyen, N.T., Cuong, T.X., 2020. Paleogene structural development of the northern Song Hong Basin and adjacent areas: Implications for the role of extrusion tectonics in basin formation in the Gulf of Tonkin. Tectonophysics 789, 1–22. https://doi.org/10.1016/j.tecto.2020.228522Huchon, P., Pichon, X.L., Rangin, C., 1994. Indochina Peninsula and the collision of India and Eurasia. Geology 22, 27–30. https://doi.org/10.1130/0091-7613(1994)022<0027:IPATCO>2.3.CO;2Hutchison, C.S., 2004. Marginal basin evolution: The southern South China Sea. Marine and Petroleum Geology 21, 1129–1148. https://doi.org/10.1016/j.marpetgeo.2004.07.002Jolivet, L., 1999. Oligocene-Miocene Bu Khang extensional gneiss dome in Vietnam: Geodynamic implications. Geology 67–70, 4.Jolivet, L., Beyssac, O., Goffé, B., Avigad, D., Lepvrier, C., Maluski, H., Thang, T.T., 2001. Oligo-Miocene midcrustal subhorizontal shear zone in Indochina. Tectonics 20, 46–57. https://doi.org/10.1029/2000TC900021Kim, Y.-S., Sanderson, D.J., 2006. Structural similarity and variety at the tips in a wide range of strike-slip faults: a review: Similarity and variety at strike-slip fault tips. Terra Nova 18, 330–344. https://doi.org/10.1111/j.1365-3121.2006.00697.xLacassin, R., Maluski, H., Leloup, P.H., Tapponnier, P., Hinthong, C., Siribhakdi, K., Chuaviroj, S., Charoenravat, A., 1997. Tertiary diachronic extrusion

and deformation of western Indochina: Structural and 40Ar/39Ar evidence from NW Thailand. Journal of Geophysical Research 102, 10,013-10,037. https://doi.org/10.1029/96JB03831Lei, C., Ren, J., Pei, J., Liu, B., Zuo, X., Liu, J., Zhu, S., 2021. Tectonics of the offshore Red River Fault: Implication of the junction of the Yinggehai and Qiongdongnan Basins. Science China Earth Sciences. https://doi.org/10.1007/s11430-020-9796-2Leloup, P.H., Arnaud, N., Lacassin, R., Kienast, J.R., Harrison, T.M., Trong, T.T.P., Replumaz, A., Tapponnier, P., 2001. New constraints on the structure, thermochronology, and timing of the Ailao Shan-Red River shear zone, SE Asia. Journal of Geophysical Research: Solid Earth 106, 6683–6732. https://doi.org/10.1029/2000JB900322Leloup, P.H., Lacassin, R., Tapponnier, P., Schärer, U., Zhong, D., Liu, X., Zhang, L., Ji, S., Trinh, P.T., 1995. The Ailao Shan-Red River shear zone (Yunnan, China), Tertiary transform boundary of Indochina. Tectonophysics, Southeast Asia Structure and Tectonics 251, 3–84. https://doi.org/10.1016/0040-1951(95)00070-4Lennie, C.R., 1968. Palynological Techniques used in New Zealand. New Zealand Journal of Geology and Geophysics 11, 1211–1221. https://doi.org/10.1080/00288306.1968.10420254Lepvrier, C., Maluski, H., Van Vuong, N., Roques, D., Axente, V., Rangin, C., 1997. Indosinian NW-trending shear zones within the Truong Son belt (Vietnam) 40Ar-39Ar Triassic ages and Cretaceous to Cenozoic overprints. Tectonophysics 283, 105–127. https://doi.org/10.1016/S0040-1951(97)00151-0Li, S., Advokaat, E.L., van Hinsbergen, D.J.J., Koymans, M., Deng, C., Zhu, R., 2017. Paleomagnetic constraints on the Mesozoic-Cenozoic paleolatitudinal and rotational history of Indochina and South China: Review and updated kinematic reconstruction. Earth-Science Reviews 171, 58–77. https://doi.org/10/gcvhvrMao, L., Foong, S.Y., 2013. Tracing ancestral biogeography of Sonneratia based on fossil pollen and their probable modern analogues. Palaeoworld, Neogene Climate and Environmental Evolution in Eastern Eurasia 22, 133–143. https://doi.org/10.1016/j.palwor.2013.09.002Mazur, S., Green, C., Stewart, M.G., Whittaker, J.M., Williams, S., Bouatmani, R., 2012. Displacement along the Red River Fault constrained by extension estimates and plate reconstructions. Tectonics 31. https://doi.org/10.1029/2012TC003174Minh N.B., 2014. Geological structure and tectonic evolution of the Song Ca fault zone and adjacent areas. PhD Thesis. Hanoi University of Science, Hanoi.Minh, N.B., Vuong, N.V., Tich, V.V., 2012. Features of tectonic deformation stages of the Ca river Fault Zone. Tạp Chí Địa Chất 330, 1–11.Morley, C.K., 2013. Discussion of tectonic models for Cenozoic strike-slip fault-affected continental margins of mainland SE Asia. Journal of Asian Earth Sciences 76, 137–151. https://doi.org/10.1016/j.jseaes.2012.10.019Morley, C.K., Charusiri, P., M Watkinson, I., 2011. Structural geology of Thailand during the Cenozoic Modern tectonic setting of Thailand. Geology of Thailand. 273–334.Morley, R.J., 2000. Origin and Evolution of Tropical Rain Forests, 1st ed. John Wiley & Sons Ltd.Morley, R.J., 1991. Tertiary stratigraphic palynology in Southeast Asia: current status and new directions. Bulletin of the Geological Society of Malaysia 28, 1–36. https://doi.org/10.7186/BGSM28199101Morley,

R.J., 1977. Palynology of Tertiary and Quaternary Sediments in Southeast Asia. Indonesian Petroleum Association 6th Annual Convention Proceedings. Indonesian Petroleum Association, 255–276.Morley, R.J., Morley, H.P., 2013. Mid Cenozoic freshwater wetlands of the Sunda region. Journal of Limnology 72, 18–35. https://doi.org/10.4081/jlimnol.2013.s2.e2Muller, J., 1968. Palynology of the Pedawan and Plateau Sandstone Formations (Cretaceous-Eocene) in Sarawak, Malaysia. Micropaleontology 14, 1–37. https://doi.org/10.2307/1484763Nagy, E.A., Schärer, U., Minh, N.T., 2000. Oligo-Miocene granitic magmatism in central Vietnam and implications for continental deformation in Indochina. Terra Nova 12, 67–76. https://doi.org/10.1111/j.1365-3121.2000.00274.xNielsen, L.H., Petersen, H.I., Thai, N.D., Duc, N.A., Fyhn, M.B.W., Boldreel, L.O., Tuan, H.A., Lindström, S., Hien, L.V., 2007. A Middle–Upper Miocene fluvial–lacustrine rift sequence in the Song Ba Rift, Vietnam: an analogue to oil-prone, small-scale continental rift basins. Petroleum Geoscience 13, 145–168. https://doi.org/10.1144/1354-079307-748Palin, R.M., Searle, M.P., Morley, C.K., Charusiri, P., Horstwood, M.S. a, Roberts, N.M.W., 2013. Timing of metamorphism of the Lansang gneiss and implications for left-lateral motion along the Mae Ping (Wang Chao) strike-slip fault, Thailand. Journal of Asian Earth Sciences 76, 120–136. https://doi.org/10.1016/j.jseaes.2013.01.021Pubellier, M., Morley, C.K., 2014. The basins of Sundaland (SE Asia): Evolution and boundary conditions. Marine and Petroleum Geology 58, 555–578. https://doi.org/10.1016/j.marpetgeo.2013.11.019Rangin, C., Klein, M., Roques, D., Le Pichon, X., Trong, L.V., 1995. The Red River fault system in the Tonkin Gulf, Vietnam. Tectonophysics 243, 209–222. https://doi.org/10.1016/0040-1951(94)00207-PRiding, J.B., Kyffin-Hughes, J.E., 2004. A review of the laboratory preparation of palynomorphs with a description of an effective non-acid technique. Revista Brasileira de Paleontologia 7, 13–44. https://doi.org/10.4072/rbp.2004.1.02Schmidt, W.J., Hoang, B.H., Handschy, J.W., Hai, V.T., Cuong, T.X., Tung, N.T., 2019. Tectonic evolution and regional setting of the Cuu Long Basin, Vietnam. Tectonophysics. https://doi.org/10.1016/j.tecto.2019.03.001Tapponnier, P., Peltzer, G., Armijo, R., 1986. On the mechanics of the collision between India and Asia. Geological Society, London, Special Publications 19, 113–157. https://doi.org/10.1144/GSL.SP.1986.019.01.07Thanh, T.D., Khuc, V., 2011. Stratigraphic units of Vietnam, 2nd ed. Vietnam National University Publisher, Hanoi.Thom, B.V., 2004. Neotectonics and modern tectonics characteristics of the Rao Nay fault. Tạp Chí Địa Chất 285, 98–107.Thom, B.V., Yem, N.T., Hung, N.V., 2013. Song Ca fault zone with its extension in Laos territory. Journal of Geology (VN) 336–337, 79–91.Tien, P.C., Linh, N.N., Hung, L.Q., 2009. Geological map of Cambodia, Laos and Vietnam at scale 1:1,500,00. Vietnam Institute of Geosciences and Mineral Resources.Traverse, A., 2007. Differential Sorting of Palynomorphs into Sediments: Palynofacies, Palynodebris, Discordant Palynomorphs. Paleopalynology. Springer, Dordrecht, 543–579.Tri, T.V., Khuc, V., 2011. Geology and Earth Resources of Vietnam. Vietnam Public House for Science and Technology, Hanoi.Vu,

A.T., Wessel Fyhn, M.B., Xuan, C.T., Nguyen, T.T., Hoang, D.N., Pham, L.T., Van, H.N., 2017. Cenozoic tectonic and stratigraphic development of the Central Vietnamese continental margin. Marine and Petroleum Geology 86, 386–401. https://doi.org/10.1016/j.marpetgeo.2017.06.001Wang, E., Burchfiel, B.C., 1997. Interpretation of Cenozoic Tectonics in the Right-Lateral Accommodation Zone Between the Ailao Shan Shear Zone and the Eastern Himalayan Syntaxis. International Geology Review 39, 191–219. https://doi.org/10.1080/00206819709465267Zhu, M., Graham, S., McHargue, T., 2009. The Red River Fault zone in the Yinggehai Basin, South China Sea. Tectonophysics 476, 397–417. https://doi.org/10.1016/j.tecto.2009.06.015

Appendices

Appendix A: Palynological analysis of field samples

Sample KB 4: palynomorph assemblages obtained are very abundant and diverse, but the most common are taxa of mountain pollen: *Alnipollenites verus, Abiespollenites* spp.*, Piceapollenites spp., Pinuspollenites* spp.*, Tsugapollenites* spp.*, Taxodiaceae* undiff., *Bisaccatepollenites* spp., *Betulapollenites* spp., and freshwater sporomorphs: *Polypodiaceaesporites* undiff., *Acrostichum aureun*, *Florschuetzia trilobata.* The age of the sample is in the Early-Middle Miocene based on the abundance of *Florschuetzia trilobata* last appeared at the end of the Middle Miocene, and the extreme abundance of *Alnipollenites* pollen that was only abundant during the Miocene in Vietnam. Furthermore, no Oligocene marker palynomorphs were found.

Sample DP 2-3: palynomorph taxa were abundant, mainly belonging to swamp taxa and freshwater spores: *Polypodiaceaesporites* undiff., *Polypodiisporites perverrucatus*, *Stenochlaena palustris*, *Lygodiumsporites* spp., *Pterisisporites* (psilate) spp. The age of the sample is in the Early-Middle Miocene based on the presence of *Florschuetzia levipoli* that first appeared at the beginning of the Early Miocene, and *Florschuetzia trilobata* which is not younger than the Middle Miocene.

Sample QB 2-1: Palynomorph assemblages recorded are poor, including taxa of hill and mountain origin: *Piceapollenites* spp.*, Pinuspollenites* spp., *Tsugapollenites* spp., *Bisaccatepollenites* spp., *Abiespollenites* spp., *Alnipollenites verus*, *Altingia* spp., and swamp riverine: *Polypodiisporites perverrucatus*, *Stenochlaena palustris.* The age of the sample is confined to the Miocene by the finding of *Florschuetzia levipoli* which appeared in the Early Miocene and were common in the Middle Miocene. Furthermore, no Pliocene – Quaternary marker palynomorphs such as *Podocarpus imbricatus*, *Phyllocladus* were recorded.

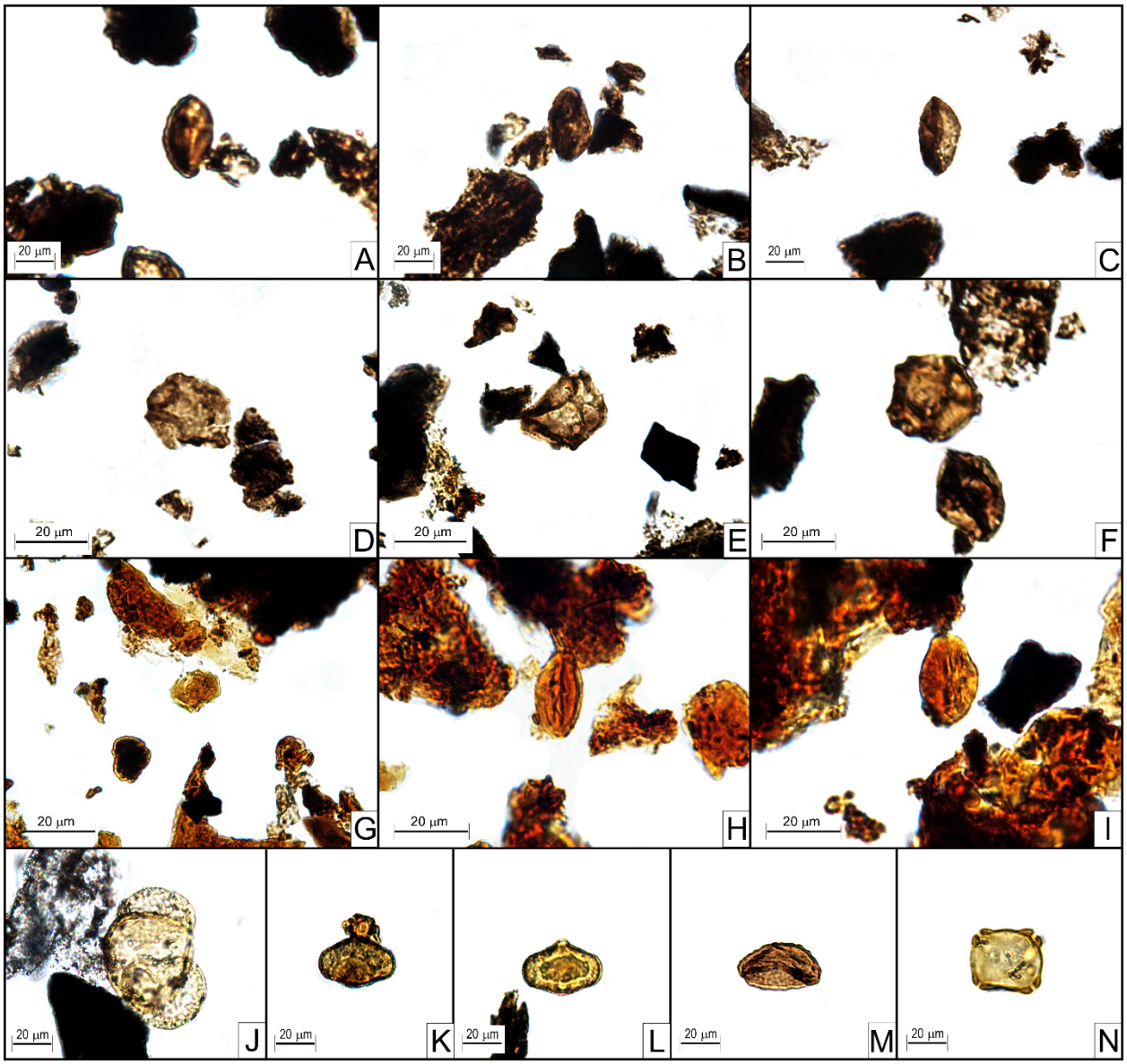

Figure A.1. Photographs of characteristic palynomorphs in analyzed samples. A) *Florschuetzia trilobata* (robust), KB 4; B & C) *Florschuetzia trilobata*, KB 4 ; D - F) *Alnipollenites verus*, KB 4; G) *Florschuetzia levipoli,* DP 2-3; H & I) *Florschuetzia trilobata,* DP 2-3; J). *Pinuspollenites* spp., QB 2-1; K & L) *Florschuetzia levipoli,* QB 2-1; M) Polypodiisporites perverrucatus, QB 2-1; N) *Alnipollenites verus*, QB 2-1.